REVIEW ARTICLE OPEN

Advances in large-scale DNA engineering with the CRISPR system

Lee Wha Gwon[1,2,6], Isabel Wen Badon[3,4,6], Youngjeon Lee[1,2], Ho-Joong Kim[5✉] and Seung Hwan Lee[3✉]

In recent years, DNA engineering technology has undergone significant advancements, with clustered regularly interspaced short palindromic repeats (CRISPR)-based target-specific DNA insertion emerging as one of the most rapidly expanding and widely studied approaches. Traditional DNA insertion technologies employing recombinases typically involve introducing foreign DNA into genes in vivo by either pre-engineering recognition sequences specific to the recombinase or through genetic crossing to incorporate the requisite recognition sequence into the target gene. However, CRISPR-based gene insertion technologies have advanced to streamline this engineering process by combining the CRISPR–Cas module with recombinase enzymes. This process enables accurate and efficient one-step insertion of foreign DNA into the target gene in vivo. Here we provide an overview of the latest developments in CRISPR-based gene insertion technologies and discusses their potential future applications.

Experimental & Molecular Medicine; https://doi.org/10.1038/s12276-025-01530-0

INTRODUCTION

As genomic research advances toward understanding complex traits and developing curative therapies, the need for large-scale genome editing tools capable of modifying hundreds to thousands of bases is rapidly growing[1,2]. Such capabilities are crucial in diverse fields including synthetic biology[3], developmental biology[4], disease modeling[5,6] and gene therapy[7], where they support applications such as multigene circuit engineering[8], reconstruction of regulatory domains[9], modification of DNA duplications[10] and rewiring of complex genetic networks underlying human diseases[11]. Traditional large-scale DNA engineering tools, such as recombinases[12], integrases[13] and resolvases[14], are enzyme classes that mediate DNA rearrangement with distinct mechanisms and roles. Recombinases (for example, Cre and Flp) enable precise site-specific modifications[15–17], integrases (for example, λ and φC31) insert viral DNA into host genomes directionally[18,19], and resolvases (for example, Tn3 and RuvC) resolve recombination intermediates to maintain genome integrity[20,21]. These tools are foundational in molecular biology, synthetic biology and gene therapy for targeted and dynamic genome editing[22–24].

The Cre-lox system, a prototypical tyrosine recombinase derived from bacteriophage P1, has become one of the most extensively utilized tools for precise genome engineering in eukaryotic and mammalian systems[25–28] (Fig. 1a and Table 1). By contrast, serine recombinases—such as Bxb1 integrase, phiC31 integrase and transposases—offer irreversible recombination with simpler mechanisms and higher efficiency across a broad range of cell types[29–32] (Fig. 1b and Table 2). These enzymes have driven advancements in genetic engineering in both prokaryotic and eukaryotic hosts[33–35], enabling the development of transgenic models, including *Drosophila*[36], zebrafish[37], medaka fish[38], mouse[39], chickens[40] and pigs[41,42]. In addition to these recombinases, which have limited target recognition, in silico approaches have identified recombinase-like sequences with novel properties[43]. Notably, IS110 family elements (IS621) demonstrate target-specific gene recombination capacity through reprogrammable bridge RNAs[44,45] (Fig. 1c). While traditional site-specific recombination systems have enabled precise DNA rearrangements, their editing capacity remains limited, largely constrained by dependence on predefined recognition sequences, relatively small target regions and low efficiency[22,46]. As a result, more versatile and scalable platforms are required to meet the demands of modern genome engineering.

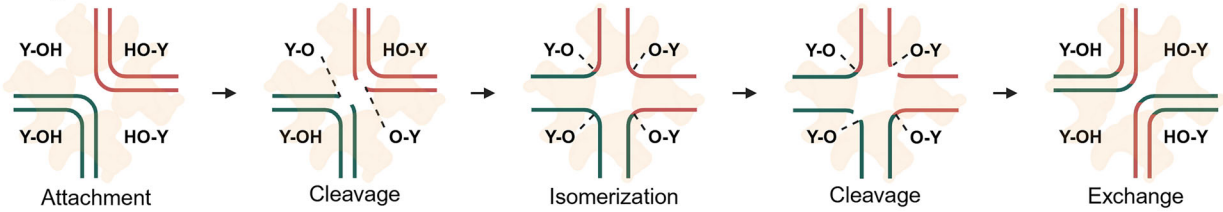## STRATEGIES FOR LARGE-SCALE DNA ENGINEERING USING EXISTING RECOMBINASES

Site-specific recombinations have been widely employed for efficient genetic manipulation[47], enabling the insertion, excision and exchange of target genes across diverse cellular and tissue contexts[17,48] (Fig. 2). Key technologies include Recombinase-Mediated Cassette Exchange (RMCE)[49], Serine and Tyrosine Recombinase-Assisted Integration of Genes for High-Throughput Investigation (STRAIGHT-IN)[46], Synthetic Chromosome Rearrangement and Modification by LoxPsym-mediated evolution (SCRaMbLE)[50,51], Serine Integrase Recombinational Assembly (SIRA)[52], Dual Integrase Cassette Exchange (DICE)[53], Serine recombinase–Assisted Genome Engineering (SAGE)[54] and Recombinase-Mediated Twin Site Targeting (RMTT) technologies[55] based on tyrosine (Fig. 2a) or

Fig. 1 Mechanisms of DNA targeting by recombinase enzymes. a, Tyrosine recombinases induce single-strand cuts in both the target and donor DNA, facilitating strand exchange and religation for recombination. The green or red marked curved lines indicate target or donor DNA, Y denotes tyrosine active residue in tyrosine recombinases and OH represents the hydroxyl residue in target or donor DNA. **b**, Serine recombinases create double-strand breaks in the target and donor DNA. Through domain rotation within the recombinase, cleave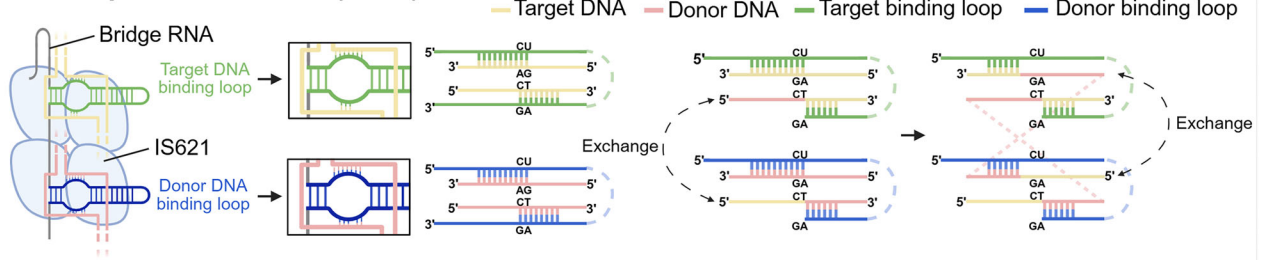d DNA strands are rotated and religated, enabling DNA recombination. The green or red marked lines indicate target or donor DNA, S denotes serine active residue in serine recombinases and OH represents the hydroxyl residue in target or donor DNA. **c**, The transposable element, IS621 recognizes its target using a complementary bridge RNA without requiring a landing pad sequence. It induces DNA cleavage and mediates recombination in a manner similar to tyrosine recombinases, involving single-strand cuts, strand exchange and religation. The yellow and pink lines represent the target DNA and donor DNA, and the green and blue stemloops represent the target binding loop and donor binding loop of bridge RNA, respectively.

Table 1. Cre and other site-specific tyrosine recombinases.

Recombinase module	Source organism	Function	PDB ID	References
Cre	Bacteriophage P1	Genetic excision, inversion and translocation	1NZB	150
XerA, XerC, XerD and XerH	XerA: *Thermoplasma acidophilum DSM 1728* XerC: *Pyrococcus abyssi* XerD: *Escherichia coli* XerH: *Helicobacter pylori 26695*	Excision: dimer reduction in the E. coli chromosome as well as in many other bacterial chromosomes and some plasmids	XerA: 5HXY XerC: 4A8E XerD: 1A0P XerH: 5JK0	XerA[151] XerC — XerD[152] XerH[153]
XisA and XisC	*Enterococcus faecalis*	Excision: for developmentally regulated gene activation in Anabaena	1Y6U	154

Each recombinase is listed with its source organism, primary function, corresponding PDB (https://www.rcsb.org/) deposit ID (if available) and relevant references. A dash indicates that the information is not available or not applicable.

serine (Fig. 2b) recombinases. However, the reliance on DNA recognition site 'landing pad sequence' for recombinase function in the mammalian cell environment limits their wide application in biomedical and therapeutic research[43]. Traditional recombination-based approaches, such as the Cre-lox system, exhibit site specificity but lack programmability and guide RNA dependency. Despite their widespread application, including in in vivo studies, there remains a critical need to develop next-generation technologies that are programmable and guided by RNA, thereby enabling more precise and flexible genome engineering.

ADVANCES IN TARGET-SPECIFIC DNA MODIFICATION USING RNA-GUIDED CRISPR SYSTEM
To address the limitations of existing recombinases, DNA modification technologies are being developed such that they

Table 2. BxbI and other site-specific serine recombinases.

Recombinase module	Source organism	Function	PDB ID	Reference
BxbI	*Mycobacterium smegmatis*	Phage BxbI integrase	—	—
A118	*Listeria*	Phage A118 integrase	4KIS	155
phiC31	*Streptomyces*	Phage phiC31 integrase	4BQQ	—
TP901	*Lactococcus*	Phage TP901-1 integrase	3BVP	156
phiRV1	*Mycobacterium tuberculosis*	Prophage-like element integrase	6LG3	157
TnpX	*Clostridium*	Integrative mobile element Tn4451 transposase	2MHC	158

Each recombinase is listed with its source organism, primary function, corresponding PDB (https://www.rcsb.org/) deposit ID (if available) and relevant references. A dash indicates that the information is not available or not applicable.
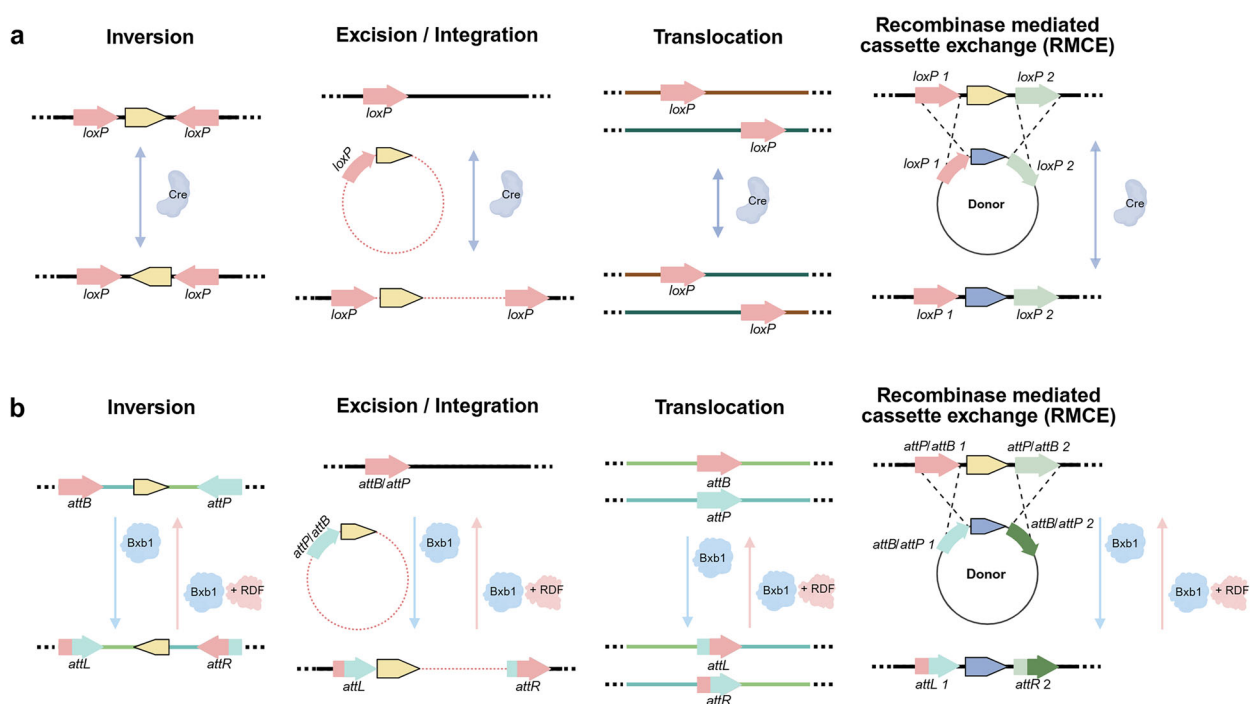

Fig. 2   Large-scale DNA editing using recombinase enzymes. a, Tyrosine recombinases (representative enzyme, Cre) require recognition of short sequences such as loxP (recognition sequence for Cre recombinase) for target DNA and donor DNA recombination. These sequences, with palindromic structures, remain unchanged after recombination. Depending on the orientation and location of the recognition sites, tyrosine recombinases can perform inversions, excisions, integrations, translocations and cassette exchanges. loxP1 and loxP2 represent different types of loxP recognition sequence. **b,** Serine recombinases (representative enzyme, BxbI) recognize *attB/attP* sequences in the target or donor DNA, respectively. Following unidirectional recombination, the hybrid sequences attL and attR are formed. Similar to tyrosine recombinases, serine recombinases enable large-scale DNA editing, including inversions, excisions, integrations, translocations and cassette exchanges, based on the orientation and location of recognition sequences (*attB/attP*). RDF, recombination directionality factor; RMCE, recombinase-mediated cassette exchange.

can be reprogrammed to target DNA using target-specific DNA binding modules[56]. Among these, the clustered regularly interspaced short palindromic repeats (CRISPR) system is the most widely used owing to its accuracy and the ease of fabricating guide RNAs to match target DNA[57–59] (Fig. 3). CRISPR systems are classified into class I (types I, III and IV), which require multiple Cas components, and class II (types II, V and VI), which use a single Cas enzyme. These CRISPR systems require a mature CRISPR RNA and trans-activating RNA for target recognition and cleavage[58]. To facilitate genome editing, RNA-guided CRISPR effectors are employed to induce DNA double-strand breaks (DSBs) at specific sites, leveraging DNA repair mechanisms to copy donor DNA sequences into the target genome[60,61] (Fig. 3a–c). To enhance homology-directed repair (HDR) efficiency (Fig. 3b), strategies have been developed, including engineering CRISPR effectors, optimizing donor DNA design and suppressing the non-

homologous end-joining (NHEJ) pathway using small molecules, enabling the knock-in of large DNA fragments into target genes[62–69]. The HDR depends on cell cycle, it is only positive in S or G2 phase and also generate indel mutations caused by DNA double-strand breaks and following the NHEJ pathway. Alternatively, technologies such as homology-independent targeted insertion (HITI) have emerged (Fig. 3c), which simultaneously induce DSBs at endogenous sites within cells and in donor DNA, facilitating DNA fragment insertion via the NHEJ pathway[70,71]. The HITI method does not only depend on the cell cycle but also generates indel mutations dominantly, which is a critical limitation. Despite their efficacy, these methods rely on the DSB-inducing capabilities of CRISPR effectors, which inherently carry challenges such as off-target effects and unintended DNA modifications at on-target sites[72]. Recent advancements have focused on using modified forms of CRISPR–Cas effectors, such as
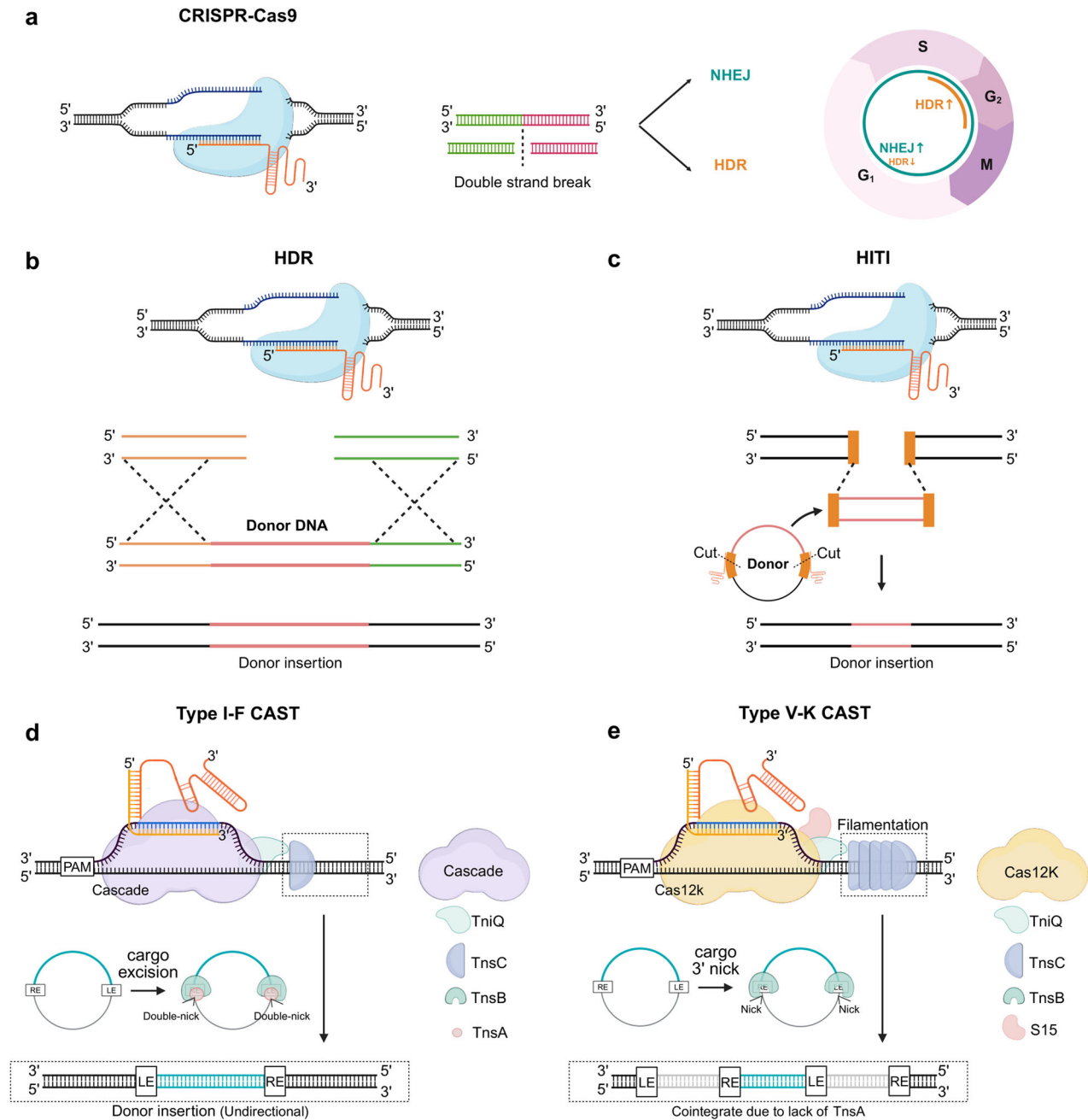
Fig. 3 Large-scale DNA engineering strategies utilizing CRISPR systems, either through the induction of double-strand breaks or via DNA break-free approaches. a, The CRISPR–Cas9 system induces double-strand breaks in target DNA using reprogrammed guide RNAs, enabling effective genome editing through DNA repair pathways such as NHEJ or homology-directed repair (HDR). The activation of each DNA repair pathway is intricately regulated in a cell-cycle-dependent manner, with distinct mechanisms predominating at specific phases. **b**, HDR enables high-fidelity integration of donor DNA by leveraging homology arms that are complementary to the genomic regions flanking the target locus, facilitating sequence-specific recombination. **c**, Homology-independent targeted integration (HITI) achieves targeted donor DNA insertion through the NHEJ pathway. The donor template is designed to contain sequences identical to the endogenous cleavage site, thereby enabling orientation-specific and precise integration. **d**, Type I-F CRISPR-associated transposase (CAST) enables double-strand break-free genomic integration via a multisubunit cascade complex that recognizes the target DNA through a CRISPR RNA (crRNA). Upon target engagement, the ATP-dependent recruitment of TnsC facilitates the bridging of the cascade complex to the transposition machinery. The target site of the donor DNA is accurately recognized and precisely cleaved by TnsA and TnsB, thereby allowing unidirectional integration at the target locus through a single TnsC-dependent mechanism. **e**, Type V-K CAST utilizes a single-effector Cas12k protein to mediate crRNA-guided target recognition. In the absence of TnsA, complete excision of the donor DNA is precluded, resulting in integration through a cointegration mechanism. TnsC assembles into ATP-dependent filaments along the DNA substrate, promoting accurate target site selection and stabilizing the integration process. LE, left end; RE, right end. The figures were created using BioRender software (BioRender.com).

Table 3. CRISPR-based large-scale DNA modification system.

Name	Recombinase system (mutant type)	Deleted or substituted gene size (bp), efficiency (%)	Inserted gene size (bp), efficiency (%)	Delivery method (target organism)	Reference
CAST (type I-F)	PseCAST	–	~1.3 kb, ~ 1% (cell line)	Lipofection (HEK293T cell lines)	[101]
CAST (type V-K)	MG64-1	–	~3.6 kb, < 1% (cell lines)	Lipofection (K562, HEK293T cell lines)	[102]
evoCAST (type I-F)	Evolved PseCAST: TnsA (P88T, I147V, V170L, F180L, F182L), TnsB (F43S, Y349N, P352T, A390V, D396N, Q410K, H464R, V526E, Q549R, Q594L), TnsC (R197, N314K), Cas7 (A347K) and Cas8 (N125D, A244N, A410R)	–	~ 4.7 kb, ~15% (cell line)	Lipofection (HEK293T, HeLa, HuH7 cell line)	[103]
PRIME-Del	–	Deletion, ~10 kb, 1-30% (cell line)	–	Lipofection or Lentiviral (HEK293T cell line)	[121]
TJ-PE	–	Substitution, 74 bp, average 2.5% (mice)	~500 bp, ~ 11.4% (cell line)	Lipofection (HEK293T cell line, Fah mutant B6/Tyr- mice)	[120]
Twin-prime editing (twinPE)	–	Deletion ~818 bp, Inversion ~40 kb (cell line)	Maximum size 113 bp, ~10% (cell line)	Lipofection (HEK293T cell line)	[118]
PASTE	WT Bxb1	–	~36 kb	AAV or AdV delivery	[126]
PASSIGE	WT Bxb1	–	~3 kb	lipofection	[127]
evoPASSIGE	evoBxb1 (V74A)	–	~10.5 kb	lipofection	[127]
eePASSIGE	eeBxb1 (V74A, E229K and V375I)	–	~10.5 kb	lipofection	[127]
PE (with hyperactive integrase)	Hyperactive PhiC31	–	~6.6 kb	lipofection, electroporation	[128]
PE (with hyperactive integrase)	Hyperactive Bxb1 (I87L, H95Y, V122M, A369P and E434G)	–	~15.7 kb	lipofection, electroporation	[128]

Each CRISPR-based technology is listed according to the recombinase system utilized, the type of editing outcome (deletion, substitution or insertion), editing efficiency, target organism and the corresponding reference. A dash indicates that the information is not available or not applicable.

nickases or inactivated versions, to enhance homology-directed repair and enable more precise DNA insertion while minimizing associated risks[73,74]. Recently, on the other hand, gene editing using transposon systems associated with CRISPR has also been reported (Fig. 3d,e and Table 3). In 2017, Peters et al. uncovered CRISPR elements work with Tn7-like transposons[75]. CASTs are RNA-guided elements that integrate into DNA by base-pairing target protospacers with complementary CRISPR RNA spacers and recognizing protospacer adjacent motifs (PAMs)[75,76]. In additon, CAST systems utilize the conserved DDE-family transposase TnsB, which catalyzes strand transfer during transposition, together with accessory factors TnsC and TniQ[77]. These systems have been identified and developed from diverse bacterial strains[78,79]. So far, several CAST subtypes—namely I-C, I-D, I-E, I-F, IV-A and V-K—have been identified, among which subtypes I-F and V-K are the most well-characterized[80–83]. The type I-F CAST system encodes Cas6, Cas7 and Cas8, which together form the Cascade complex, and facilitates efficient insertion of genetic elements by employing an RNA-guided DNA cut-and-paste transposition mechanism[78,84,85] (Fig. 3d). The cascade and guide RNA, together with TniQ which recruit TnsC, directs target DNA recognition, while TnsA, TnsB and TnsC form a heteromeric transposase complex that catalyzes DNA cleavage and transposition[78,86]. DNA integration by type I-F CASTs occurs approximately ~50 bp downstream of the target site[85]. In type V-K CAST systems (Fig. 3e), transposition is orchestrated by the single-effector protein Cas12k, with DNA integration occurring 60–66 base pairs downstream of the PAM site[79]. Unlike the type I-F CAST system, the type V-K CAST mechanism generates cointegrate products through a replicative pathway, owing to the absence of the endonuclease TnsA[85,87]. To enable successful DNA transposition, the TniQ factor and ribosomal protein S15 are additionally recruited[88], promoting the TniQ-mediated assembly of TnsC into a filamentous structure along the target DNA. This arrangement facilitates subsequent interaction with TnsB, thereby culminating in the formation of the complete integration complex[89].

CAST systems present a unique strategy for integrating large genetic elements into specific genomic loci without introducing double-strand breaks, relying solely on guide RNA for target recognition. In various prokaryotic hosts, this method has demonstrated nearly complete insertion in *Escherichia coli*, enabling the stable integration of donor sequences up to approximately 15.4 kb with type I-F CAST[90–95] and as much as 30 kb using type V-K variants[79,96–100]. Despite these successes, applications in mammalian cells are still in early stages (Table 3). Type I-F CAST, for example, has only achieved about 1% editing efficiency in HEK293 cell line with approximately 1.3 kb sized donor DNA[101]. As another example, to facilitate large-scale DNA editing in human-derived cells, a V-K CAST variant incorporating a fusion protein (nAnil-TnsB) was codelivered with a 2.6 kb donor DNA containing the nAnil recognition sequence[99]. As a result, a large-scale DNA editing efficiency of up to 0.06% was observed in HEK293T cells targeting plasmid DNA. Fortunately, substantial progress has been made through various biological approaches, yielding promising results for the future application of CAST systems in humans. Notably, the V-K CAST system MG64-1 was identified via metagenomic mining[102]. In HEK293 cells, this system achieved approximately 3% integration efficiency of a 3.2 kb donor at the AAVS1 locus, and integration rates of ~3% and <0.05% for a 3.6 kb therapeutic donor in K562 and Hep3B cells, respectively. More recently, a PseCAST system engineered through directed evolution has exhibited considerable potential for future use in complex biological contexts[103].

RECENT ADVANCES IN PRIME EDITING TECHNOLOGY AND ITS APPLICATION IN LARGE-SCALE DNA MODIFICATION
Prime editing is a technological advancement designed to enable the precise insertion of desired genes into target DNA in living organisms using a CRISPR-based approach[58,104–106] (Fig. 4a). This technology links a CRISPR–Cas9 module to a reverse transcriptase (RT) enzyme[107], enabling targeted DNA editing—such as base modifications, including insertions, deletions and substitutions of up to a few base pairs—guided by reprogrammed prime editing guide RNA (pegRNA)[108–110]. Since its first description in the year 2019[104], prime editors have been continuously developed and optimized to increase editing efficiency[111]. For example, prime editor version 2 (PE2) version demonstrates precise editing in human-derived cell lines without inducing DSBs[112]. To enhance the incorporation of edits, the PE3 version introduces an additional nick in the target strand, promoting base excision repair (Fig. 4b). However, the additional nicking induced in the target strand can result in inefficiencies in various human-derived cell targets and induce unintended modifications, including insertions and deletions[104,113,114]. To address these issues, the PE4 and PE5 systems were developed, which significantly improve prime editing efficiency by combining PE2 and PE3 system with transient expression of a dominant-negative form of MLH1, which is a mismatch repair-related protein[115] (Fig. 4c,d). Further advancements, such as the PE6a, PE6b and PE6c systems, use mutated evo-Ec48 and evo-Tf1 as RTs[116] (Fig. 4e). Moreover, PE6d incorporates RNaseH-truncated and engineered Moloney murine leukemia virus (M-MLV) RTs. Further mutations to the CRISPR–Cas9 module have led to the development of PE6e-g, showing increased editing efficiency[116]. Integrating a small RNA-binding La protein to generate PE7 enhanced prime editing efficiency by up to 21.2-fold while reducing on-target insertions and deletions[117] (Fig. 4f). The endogenous La protein binds to poly-uridine tracts in RNAs, protecting them from exonuclease degradation of 3′ end of pegRNA′. Notably, multiple paired prime editing strategies (Fig. 4g and Table 3), including twin-prime editing (twinPE)[118], bi-direction prime editing (Bi-PE)[119], template-jumping prime editing (TJ-PE, sequential utilization of two pegRNAs enables the linkage of two distal genomic loci, facilitating insertions or exon replacement)[120] and PRIME-Del (the intervening sequence is completely removed, followed by seamless ligation of the flanking homology arms)[121], have been developed to enable the simultaneous editing of both DNA strands, thereby enhancing the overall efficiency and precision of large-scale DNA modifications, such as deletion, insertion and substitution in target cell lines. Another technique that improves the efficiency of prime editing involves the engineering of prime editing components, including nickases and RTs[122], which can be conjugated together or split depending on the delivery vehicles such as adeno-associated virus (AAV)[123–125]. Programmable addition via site-specific targeting elements (PASTE) technology is an optimized method for large gene insertion via prime editing[126] (Fig. 4h,j and Table 3). This approach enables large gene incorporation with high target specificity, and minimal double-strand breaks, by sequentially activating target site priming via prime editors and donor DNA insertion mediated by site-specific recombinases. PASTE technology utilizes the same components as prime editing, with the addition of Bxb1 integrase tethered to M-MLV RT. Moreover, the pegRNA of prime editing is extended with a landing pad (*attB* sequence) for Bxb1 recognition[126–128]. In this case, PASTE efficiency depends on target loci and pegRNA parameters (length of PBS, RT and *attB* sequences). According to the findings validated so far, the PASTE system allows the directed integration of large sequences (~36 kb) to target sites using serine integrase[126–128].

Following the recent development of PASTE technology, which integrates recombinases with prime editing, various studies have focused on improving large gene insertion efficiency by engineering recombinase enzymes[127,128]. One such advancement, prime-assisted site-specific integrase gene editing (PASSIGE) technology, uses twin-prime editing to insert attP/B sites for Bxb1 binding, followed by foreign DNA insertion into the target using the highly efficient Bxb1 recombinase (Bxb1 is either coexpressed with the
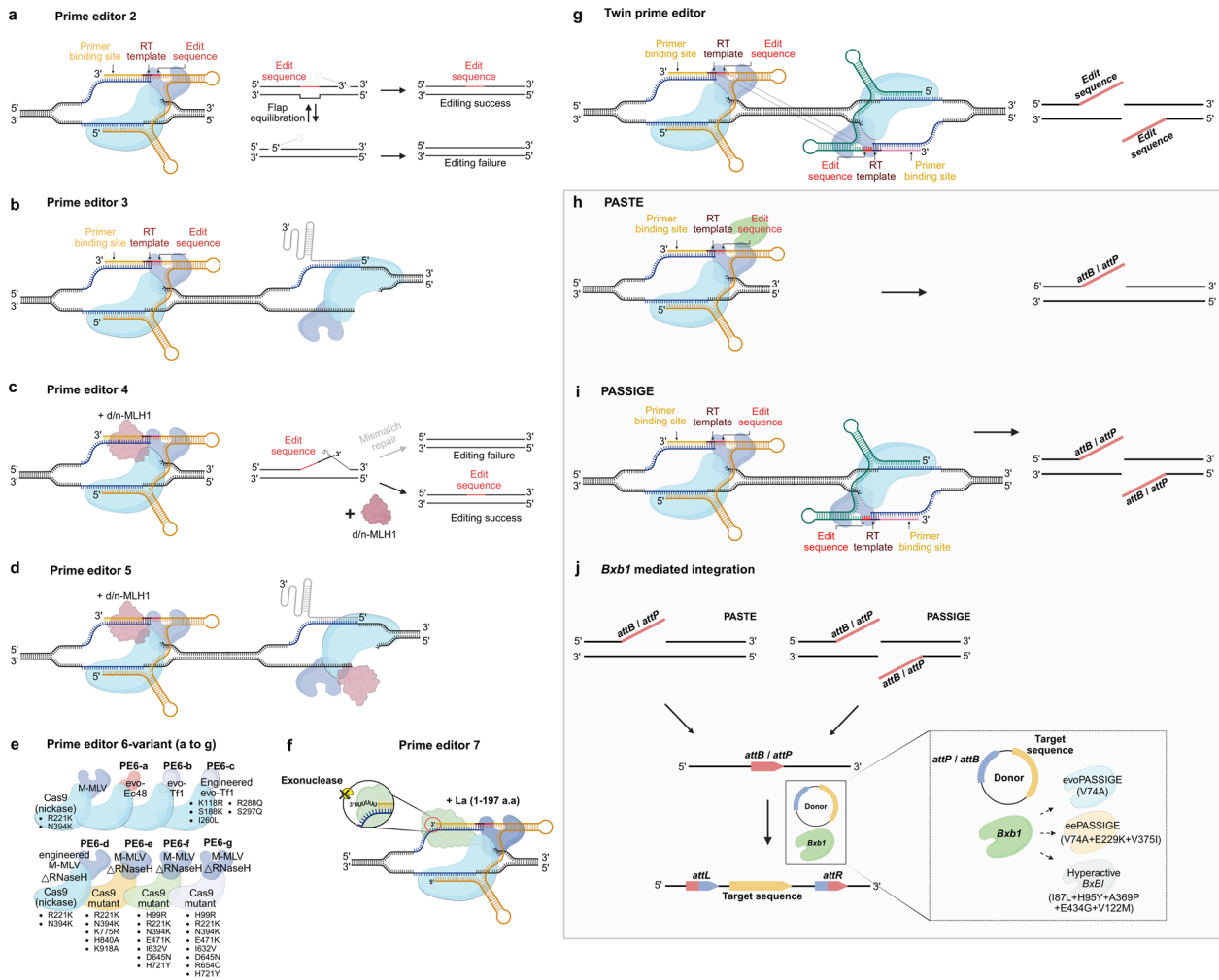
Fig. 4 Large-scale DNA editing using prime editing-based technologies. a, Prime editing employs CRISPR nickases to introduce nicks instead of double-strand breaks. An RT copies pegRNA information into the target DNA, enabling precise deletions, insertions and substitutions. PE2 utilizes pegRNA and a single CRISPR nickase-RT system. The extended 3′-flap DNA, derived from the pegRNA template, undergoes an equilibrium state of association and dissociation with the target DNA, thereby enabling the induction of the intended gene mutation through mismatch repair (MMR) mechanisms. **b**, PE3 enhances editing efficiency by introducing an additional nick opposite the non-target strand nick of the PE to control DNA substitution mediated by base excision repair. **c,d**, PE4 (**c**) and PE5 (**d**) improved PE2 and PE3, respectively, by adding functional domains to the prime editor (PE). Using a dominant-negative MLH1 (d/n-MLH1) protein disrupts the MMR complex, preventing MMR repair and enhancing desired sequence insertion. **e**, PE6 integrates a compact, optimized RT into the PE, improving editing efficiency in a smaller construct. **f**, PE7 uses the human-derived La protein to stabilize pegRNA by protecting its 3′-end tail from exonuclease degradation, enhancing editing efficiency. **g**, Twin-prime editing employs two PEs to form complementary strands via RT synthesis, enabling precise insertion, deletion and substitution through base pairing. **h–j**, Programmable DNA modification strategies leveraging site-specific recombinases in conjunction with prime editing technology enable efficient and scalable genome engineering: the PASTE system combines recombinase with a single PE to insert recombinase recognition sequences into target DNA and subsequently facilitate donor DNA recombination (**h**); the PASSIGE system utilizes twin-prime editing to insert recombinase recognition sequences into the target DNA (**i**); and sequential donor DNA recombination is achieved using site-specific recombinase (BxbI) (**j**). The BxbI recombinase employed in this system has an enhanced version developed through directed evolution to improve recombination efficiency. d/n-MLH1, dominant-negative MLH1 protein; M-MLV, Moloney murine leukemia virus. The figures were created using BioRender software (BioRender.com).

prime editor via a self-cleaving 2A peptide within the same expression construct or individually overexpressed)[127] (Fig. 4i,j and Table 3). Evolving Bxb1 through phage-assisted continuous evolution (PACE) and phage-assisted non-continuous evolution (PANCE) introduced mutations, resulting in evolutionary PASSIGE (evoPASSIGE) and enhanced evolutionary PASSIGE (eePASSIGE), which showed 9.1-fold and 16-fold improvements in integration efficiency over the PASTE system, respectively (Fig. 4j, inset). In addition, a similar approach revealed recombinase variants that enhanced large gene insertion efficiency[128]. Hyperactive versions of Bxb1 recombinases containing specific mutations demonstrated a 3.1-fold increase compared with the wild-type recombinase.

OFF-TARGET, BYPRODUCT AND TRANSLOCATION ISSUES ASSOCIATED WITH LARGE GENE INSERTION TECHNOLOGY

The CRISPR system recognizes target DNA based on guide RNA; however, its inherent tolerance for mismatched bases between the guide RNA and DNA can lead to off-target effects. These off-target CRISPR malfunctions have been reported to cause chromosomal breaks, translocations and associated developmental defects, neurodegeneration, immunodeficiency, infertility and increased cancer susceptibility[129–131]. Similarly, prime editing technologies for large gene insertion are also susceptible to off-target activities owing to guide RNA-based target recognition[126–128]. Several methods have been developed to detect the

off-target effects of prime editing[132,133], including nDigenome-seq, which uses nCas9 H840A to generate single-strand breaks in the non-target site for off-target screening[132]. In addition, PE-tag, a cell-based assay, was developed recently to analyze prime editing off-target, showing lower off-target editing where the prime editor can operate compared with conventional Cas9 systems[133]. To minimize off-target effects, strategies to improve the target specificity of SpCas9, such as SpCas9-HF1, eSpCas9, HeFSpCas9, EvoSpCas9 and HypaCas9, can be applied[134–138]. When using prime editing for large gene insertion, off-target effects can also occur through recombination by the BxBI enzyme, which allows recognition of the pseudo-*attB* site[127,128,139]. Although current studies report minimal off-target editing effects, further validation studies are necessary to ensure safety.

CONCLUDING REMARKS

Recent advances in the discovery and application of CRISPR effectors have enabled targeted gene modifications and large DNA engineering in vivo. However, prime editing, the foundation of current large DNA engineering technologies, still requires significant improvements owing to challenges, such as low gene editing efficiency, narrow targeting scope, unpredictable insertions and deletions and off-target effects caused by guide RNA-based recognition. To overcome these issues, the components of the prime editing, Cas9 nickase (H840A), RT (M-MLV RT) and pegRNA, can be fine-tuned to facilitate target sequence insertion recognized by recombinases. Previous study shows that modifying pegRNA by adding pseudoknots improves its stability, increasing efficiency by three- to fourfold[111]. Alternatively, SpCas9 orthologs can be used as an alternative to prime editing. For example, although *Streptococcus pyogenes* Cas9 (SpCas9) recognizes the 5′-NGG-3′ sequence, engineered nucleases with minimal and flexible PAMs, such as the SpG and SpRY variants, have been developed[140–143]. Prime editors utilizing PAM-flexible Cas9 variants demonstrate expanded targeting ranges, achieving up to 51.7% prime editing activity in HEK293T cells[144]. Prime editing also can be directly induced using orthologs from *Francisella novicida* Cas9, which shows high specificity for target DNA[145]. The use of highly accurate, modular prime editing technologies could enable precise, large-scale genome editing. In addition, the CRISPR–Cas12f effector, known as a micromodule for high-efficiency human cell delivery[146–149], can also be developed as a miniaturized prime editor for AAV loading. These approaches are capable of inducing high-efficiency gene editing in both plants and animals and hold significant potential for the future development of human-targeted gene therapies. Addressing the large-scale gene editing challenges from multiple perspectives, either by improving the CRISPR components or the delivery methodology, could facilitate accurate and effective gene editing across various biological targets. These advancements offer broad application potential across various fields, particularly within human systems.

REFERENCES

1. Bartley, B. A., Beal, J., Karr, J. R. & Strychalski, E. A. Organizing genome engineering for the gigabase scale. *Nat. Commun.* **11**, 689 (2020).
2. Chari, R. & Church, G. M. Beyond editing to writing large genomes. *Nat. Rev. Genet* **18**, 749–760 (2017).
3. Gibson, D. G. et al. Creation of a bacterial cell controlled by a chemically synthesized genome. *Science* **329**, 52–56 (2010).
4. Miura, K., Matoba, S., Hirose, M. & Ogura, A. Generation of chimeric mice with spermatozoa fully derived from embryonic stem cells using a triple-target CRISPR method for Nanos3. *Dagger Biol. Reprod.* **104**, 223–233 (2021).
5. Lin, Y. et al. Application of CRISPR/Cas9 system in establishing large animal models. *Front Cell Dev. Biol.* **10**, 919155 (2022).
6. Yue, Y. et al. Extensive germline genome engineering in pigs. *Nat. Biomed. Eng.* **5**, 134–143 (2021).
7. Xue, W. et al. CRISPR-mediated direct mutation of cancer genes in the mouse liver. *Nature* **514**, 380–384 (2014).
8. De Carluccio, G., Fusco, V. & di Bernardo, D. Engineering a synthetic gene circuit for high-performance inducible expression in mammalian systems. *Nat. Commun.* **15**, 3311 (2024).
9. Liu, J. et al. Reconstruction of the gene regulatory network involved in the sonic hedgehog pathway with a potential role in early development of the mouse brain. *PLoS Comput Biol.* **10**, e1003884 (2014).
10. Zhang, R. et al. Amplification editing enables efficient and precise duplication of DNA from short sequence to megabase and chromosomal scale. *Cell* **187**, 3936–3952 e3919 (2024).
11. Ushiki, A. et al. Deletion of CTCF sites in the SHH locus alters enhancer-promoter interactions and leads to acheiropodia. *Nat. Commun.* **12**, 2282 (2021).
12. Lau, Y. H. et al. Large-scale recoding of a bacterial genome by iterative recombineering of synthetic DNA. *Nucleic Acids Res.* **45**, 6971–6980 (2017).
13. Miyazaki, R. & van der Meer, J. R. A new large-DNA-fragment delivery system based on integrase activity from an integrative and conjugative element. *Appl Environ. Microbiol* **79**, 4440–4447 (2013).
14. Wyatt, H. D. & West, S. C. Holliday junction resolvases. *Cold Spring Harb. Perspect. Biol.* **6**, a023192 (2014).
15. Andrews, B. J., Proteau, G. A., Beatty, L. G. & Sadowski, P. D. The FLP recombinase of the 2 micron circle DNA of yeast: interaction with its target sequences. *Cell* **40**, 795–803 (1985).
16. Sauer, B. & McDermott, J. DNA recombination with a heterospecific Cre homolog identified from comparison of the pac-c1 regions of P1-related phages. *Nucleic Acids Res.* **32**, 6086–6095 (2004).
17. Tian, X. & Zhou, B. Strategies for site-specific recombination with high efficiency and precise spatiotemporal resolution. *J. Biol. Chem.* **296**, 100509 (2021).
18. Landy, A. The lambda integrase site-specific recombination pathway. *Microbiol Spectr.* **3**, MDNA3-0051–2014 (2015).
19. Pokhilko, A. et al. The mechanism of varphiC31 integrase directionality: experimental analysis and computational modelling. *Nucleic Acids Res.* **44**, 7360–7372 (2016).
20. Lloyd, R. G. & Sharples, G. J. Processing of recombination intermediates by the RecG and RuvAB proteins of Escherichia coli. *Nucleic Acids Res.* **21**, 1719–1725 (1993).
21. Nicolas, E. et al. The Tn3-family of replicative transposons. *Microbiol. Spectr.* https://doi.org/10.1128/microbiolspec.MDNA3-0060-2014 (2015).
22. Gaj, T., Sirk, S. J. & Barbas, C. F. 3rd. Expanding the scope of site-specific recombinases for genetic and metabolic engineering. *Biotechnol. Bioeng.* **111**, 1–15 (2014).
23. Gaj, T. et al. Enhancing the specificity of recombinase-mediated genome engineering through dimer interface redesign. *J. Am. Chem. Soc.* **136**, 5047–5056 (2014).
24. Grindley, N. D., Whiteson, K. L. & Rice, P. A. Mechanisms of site-specific recombination. *Annu Rev. Biochem* **75**, 567–605 (2006).
25. Yarmolinsky, M. & Hoess, R. The legacy of Nat Sternberg: the genesis of Cre-lox technology. *Annu Rev. Virol.* **2**, 25–40 (2015).
26. Sternberg, N. Demonstration and analysis of P1 site-specific recombination using lambda-P1 hybrid phages constructed in vitro. *Cold Spring Harb. Symp. Quant. Biol.* **43**, 1143–1146 (1979). Pt 2.
27. Sauer, B. Functional expression of the cre-lox site-specific recombination system in the yeast *Saccharomyces cerevisiae*. *Mol. Cell Biol.* **7**, 2087–2096 (1987).
28. Sauer, B. & Henderson, N. Site-specific DNA recombination in mammalian cells by the Cre recombinase of bacteriophage P1. *Proc. Natl Acad. Sci. USA* **85**, 5166–5170 (1988).
29. Smith, M. C. & Thorpe, H. M. Diversity in the serine recombinases. *Mol. Microbiol* **44**, 299–307 (2002).
30. Kim, A. I. et al. Mycobacteriophage Bxb1 integrates into the *Mycobacterium smegmatis* groEL1 gene. *Mol. Microbiol* **50**, 463–473 (2003).
31. Zhang, Q., Azarin, S. M. & Sarkar, C. A. Model-guided engineering of DNA sequences with predictable site-specific recombination rates. *Nat. Commun.* **13**, 4152 (2022).
32. Groth, A. C., Olivares, E. C., Thyagarajan, B. & Calos, M. P. A phage integrase directs efficient site-specific integration in human cells. *Proc. Natl Acad. Sci. USA* **97**, 5995–6000 (2000).
33. Cautereels, C. et al. Orthogonal LoxPsym sites allow multiplexed site-specific recombination in prokaryotic and eukaryotic hosts. *Nat. Commun.* **15**, 1113 (2024).
34. Lloyd, J. P. B. et al. Synthetic memory circuits for stable cell reprogramming in plants. *Nat. Biotechnol.* **40**, 1862–1872 (2022).
35. Vizoso, M. et al. A doxycycline- and light-inducible Cre recombinase mouse model for optogenetic genome editing. *Nat. Commun.* **13**, 6442 (2022).

36. Frickenhaus, M., Wagner, M., Mallik, M., Catinozzi, M. & Storkebaum, E. Highly efficient cell-type-specific gene inactivation reveals a key function for the Drosophila FUS homolog cabeza in neurons. *Sci. Rep.* **5**, 9107 (2015).

37. Carney, T. J. & Mosimann, C. Switch and trace: recombinase genetics in zebrafish. *Trends Genet.* **34**, 362–378 (2018).

38. Okuyama, T. et al. Controlled Cre/loxP site-specific recombination in the developing brain in medaka fish, Oryzias latipes. *PLoS ONE* **8**, e66597 (2013).

39. Karimova, M. et al. A single reporter mouse line for Vika, Flp, Dre, and Cre-recombination. *Sci. Rep.* **8**, 14453 (2018).

40. Lee, H. J. et al. Site-specific recombination in the chicken genome using Flipase recombinase-mediated cassette exchange. *FASEB J.* **30**, 555–563 (2016).

41. Li, S. et al. Dual fluorescent reporter pig for Cre recombination: transgene placement at the ROSA26 locus. *PLoS ONE* **9**, e102455 (2014).

42. Perleberg, C., Kind, A. & Schnieke, A. Genetically engineered pigs as models for human disease. *Dis. Model Mech.* https://doi.org/10.1242/dmm.030783 (2018).

43. Durrant, M. G. et al. Systematic discovery of recombinases for efficient integration of large DNA sequences into the human genome. *Nat. Biotechnol.* **41**, 488–499 (2023).

44. Durrant, M. G. et al. Bridge RNAs direct programmable recombination of target and donor DNA. *Nature* **630**, 984–993 (2024).

45. Hiraizumi, M. et al. Structural mechanism of bridge RNA-guided recombination. *Nature* **630**, 994–1002 (2024).

46. Blanch-Asensio, A. et al. STRAIGHT-IN enables high-throughput targeting of large DNA payloads in human pluripotent stem cells. *Cell Rep. Methods* **2**, 100300 (2022).

47. Olorunniji, F. J., Rosser, S. J. & Stark, W. M. Site-specific recombinases: molecular machines for the Genetic Revolution. *Biochem J.* **473**, 673–684 (2016).

48. Abioye, J. et al. High fidelity one-pot DNA assembly using orthogonal serine integrases. *Biotechnol. J.* **18**, e2200411 (2023).

49. Turan, S. et al. Recombinase-mediated cassette exchange (RMCE): traditional concepts and current challenges. *J. Mol. Biol.* **407**, 193–221 (2011).

50. Shen, Y. et al. SCRaMbLE generates designed combinatorial stochastic diversity in synthetic chromosomes. *Genome Res* **26**, 36–49 (2016).

51. Ma, L. et al. SCRaMbLE generates evolved yeasts with increased alkali tolerance. *Micro. Cell Fact.* **18**, 52 (2019).

52. Merrick, C. A., Wardrope, C., Paget, J. E., Colloms, S. D. & Rosser, S. J. Rapid Optimization of Engineered Metabolic Pathways with Serine Integrase Recombinational Assembly (SIRA). *Methods Enzymol.* **575**, 285–317 (2016).

53. Zhu, F. et al. DICE, an efficient system for iterative genomic editing in human pluripotent stem cells. *Nucleic Acids Res.* **42**, e34 (2014).

54. Elmore, J. R. et al. High-throughput genetic engineering of nonmodel and undomesticated bacteria via iterative site-specific genome integration. *Sci. Adv.* **9**, eade1285 (2023).

55. Turan, S. et al. Expanding Flp-RMCE options: the potential of Recombinase Mediated Twin-Site Targeting (RMTT). *Gene* **546**, 135–144 (2014).

56. Gaj, T., Gersbach, C. A. & Barbas, C. F. 3rd. ZFN, TALEN, and CRISPR/Cas-based methods for genome engineering. *Trends Biotechnol.* **31**, 397–405 (2013).

57. Jinek, M. et al. A programmable dual-RNA-guided DNA endonuclease in adaptive bacterial immunity. *Science* **337**, 816–821 (2012).

58. Anzalone, A. V., Koblan, L. W. & Liu, D. R. Genome editing with CRISPR–Cas nucleases, base editors, transposases and prime editors. *Nat. Biotechnol.* **38**, 824–844 (2020).

59. Pacesa, M., Pelea, O. & Jinek, M. Past, present, and future of CRISPR genome editing technologies. *Cell* **187**, 1076–1100 (2024).

60. Chen, X. et al. Recent advances in CRISPR–Cas9-based genome insertion technologies. *Mol. Ther. Nucleic Acids* **35**, 102138 (2024).

61. Lee, S. H., Kim, S. & Hur, J. K. CRISPR and target-specific DNA endonucleases for efficient DNA knock-in in eukaryotic genomes. *Mol. Cells* **41**, 943–952 (2018).

62. Gutschner, T., Haemmerle, M., Genovese, G., Draetta, G. F. & Chin, L. Post-translational regulation of Cas9 during G1 enhances homology-directed repair. *Cell Rep.* **14**, 1555–1566 (2016).

63. Aird, E. J., Lovendahl, K. N., St Martin, A., Harris, R. S. & Gordon, W. R. Increasing Cas9-mediated homology-directed repair efficiency through covalent tethering of DNA repair template. *Commun. Biol.* **1**, 54 (2018).

64. Lee, K. et al. Synthetically modified guide RNA and donor DNA are a versatile platform for CRISPR–Cas9 engineering. *eLife* https://doi.org/10.7554/eLife.25312 (2017).

65. Lin, S., Staahl, B. T., Alla, R. K. & Doudna, J. A. Enhanced homology-directed human genome engineering by controlled timing of CRISPR/Cas9 delivery. *eLife* **3**, e04766 (2014).

66. Auer, T. O., Duroure, K., De Cian, A., Concordet, J. P. & Del Bene, F. Highly efficient CRISPR/Cas9-mediated knock-in in zebrafish by homology-independent DNA repair. *Genome Res.* **24**, 142–153 (2014).

67. Charpentier, M. et al. CtIP fusion to Cas9 enhances transgene integration by homology-dependent repair. *Nat. Commun.* **9**, 1133 (2018).

68. Bae, S., Kweon, J., Kim, H. S. & Kim, J. S. Microhomology-based choice of Cas9 nuclease target sites. *Nat. Methods* **11**, 705–706 (2014).

69. Maruyama, T. et al. Increasing the efficiency of precise genome editing with CRISPR–Cas9 by inhibition of nonhomologous end joining. *Nat. Biotechnol.* **33**, 538–542 (2015).

70. Meng, X. et al. In vivo genome editing via CRISPR/Cas9-mediated homology-independent targeted integration for Bietti crystalline corneoretinal dystrophy treatment. *Nat. Commun.* **15**, 3773 (2024).

71. Suzuki, K. et al. In vivo genome editing via CRISPR/Cas9 mediated homology-independent targeted integration. *Nature* **540**, 144–149 (2016).

72. Kosicki, M., Tomberg, K. & Bradley, A. Repair of double-strand breaks induced by CRISPR–Cas9 leads to large deletions and complex rearrangements. *Nat. Biotechnol.* **36**, 765–771 (2018).

73. Richardson, C. D., Ray, G. J., DeWitt, M. A., Curie, G. L. & Corn, J. E. Enhancing homology-directed genome editing by catalytically active and inactive CRISPR–Cas9 using asymmetric donor DNA. *Nat. Biotechnol.* **34**, 339–344 (2016).

74. Wang, C. et al. dCas9-based gene editing for cleavage-free genomic knock-in of long sequences. *Nat. Cell Biol.* **24**, 268–278 (2022).

75. Peters, J. E., Makarova, K. S., Shmakov, S. & Koonin, E. V. Recruitment of CRISPR–Cas systems by Tn7-like transposons. *Proc. Natl Acad. Sci. USA* **114**, E7358–E7366 (2017).

76. Klompe, S. E. et al. Evolutionary and mechanistic diversity of Type I-F CRISPR-associated transposons. *Mol. Cell* **82**, 616–628 e615 (2022).

77. Gelsinger, D. R. et al. Bacterial genome engineering using CRISPR-associated transposases. *Nat. Protoc.* **19**, 752–790 (2024).

78. Klompe, S. E., Vo, P. L. H., Halpin-Healy, T. S. & Sternberg, S. H. Transposon-encoded CRISPR–Cas systems direct RNA-guided DNA integration. *Nature* **571**, 219–225 (2019).

79. Strecker, J. et al. RNA-guided DNA insertion with CRISPR-associated transposases. *Science* **365**, 48–53 (2019).

80. Chen, C. et al. Expanding the frontiers of genome engineering: A comprehensive review of CRISPR-associated transposons. *Biotechnol. Adv.* **78**, 108481 (2025).

81. Faure, G. et al. Modularity and diversity of target selectors in Tn7 transposons. *Mol. Cell* **83**, 2122–2136 e2110 (2023).

82. Rybarski, J. R., Hu, K., Hill, A. M., Wilke, C. O. & Finkelstein, I. J. Metagenomic discovery of CRISPR-associated transposons. *Proc. Natl Acad. Sci. USA* https://doi.org/10.1073/pnas.2112279118 (2021).

83. Shmakov, S. et al. Diversity and evolution of class 2 CRISPR–Cas systems. *Nat. Rev. Microbiol* **15**, 169–182 (2017).

84. Halpin-Healy, T. S., Klompe, S. E., Sternberg, S. H. & Fernandez, I. S. Structural basis of DNA targeting by a transposon-encoded CRISPR–Cas system. *Nature* **577**, 271–274 (2020).

85. Vo, P. L. H., Acree, C., Smith, M. L. & Sternberg, S. H. Unbiased profiling of CRISPR RNA-guided transposition products by long-read sequencing. *Mob. DNA* **12**, 13 (2021).

86. Choi, K. Y., Spencer, J. M. & Craig, N. L. The Tn7 transposition regulator TnsC interacts with the transposase subunit TnsB and target selector TnsD. *Proc. Natl Acad. Sci. USA* **111**, E2858–E2865 (2014).

87. Saito, M. et al. Dual modes of CRISPR-associated transposon homing. *Cell* **184**, 2441–2453 e2418 (2021).

88. Schmitz, M., Querques, I., Oberli, S., Chanez, C. & Jinek, M. Structural basis for the assembly of the type V CRISPR-associated transposon complex. *Cell* **185**, 4999–5010 e4917 (2022).

89. Park, J. U. et al. Structural basis for target site selection in RNA-guided DNA transposition systems. *Science* **373**, 768–774 (2021).

90. Pechenov, P. Y., Garagulya, D. A., Stanovov, D. S. & Letarov, A. V. New effective method of *Lactococcus* genome editing using guide RNA-directed transposition. *Int. J. Mol. Sci.* https://doi.org/10.3390/ijms232213978 (2022).

91. Rubin, B. E. et al. Species- and site-specific genome editing in complex bacterial communities. *Nat. Microbiol* **7**, 34–47 (2022).

92. Vo, P. L. H. et al. CRISPR RNA-guided integrases for high-efficiency, multiplexed bacterial genome engineering. *Nat. Biotechnol.* **39**, 480–489 (2021).

93. Yang, S. et al. Orthogonal CRISPR-associated transposases for parallel and multiplexed chromosomal integration. *Nucleic Acids Res.* **49**, 10192–10202 (2021).

94. Yang, S. et al. RNA-guided DNA transposition in *Corynebacterium glutamicum* and *Bacillus subtilis*. *ACS Synth. Biol.* **12**, 2198–2202 (2023).

95. Zhang, Y. et al. Multicopy chromosomal integration using CRISPR-associated transposases. *ACS Synth. Biol.* **9**, 1998–2008 (2020).

96. Chen, W. et al. Targeted genetic screening in bacteria with a Cas12k-guided transposase. *Cell Rep.* **36**, 109635 (2021).

97. Cheng, Z. H. et al. Repurposing CRISPR RNA-guided integrases system for one-step, efficient genomic integration of ultra-long DNA sequences. *Nucleic Acids Res.* **50**, 7739–7750 (2022).

98. Cui, Y. et al. A versatile Cas12k-based genetic engineering toolkit (C12KGET) for metabolic engineering in genetic manipulation-deprived strains. *Nucleic Acids Res.* **50**, 8961–8973 (2022).

99. Tou, C. J., Orr, B. & Kleinstiver, B. P. Precise cut-and-paste DNA insertion using engineered type V-K CRISPR-associated transposases. *Nat. Biotechnol.* **41**, 968–979 (2023).

100. Yap, Z. L., Rahman, A., Hogan, A. M., Levin, D. B. & Cardona, S. T. A CRISPR–Cas-associated transposon system for genome editing in Burkholderia cepacia complex species. *Appl Environ. Microbiol* **90**, e0069924 (2024).

101. Lampe, G. D. et al. Targeted DNA integration in human cells without double-strand breaks using CRISPR-associated transposases. *Nat. Biotechnol.* **42**, 87–98 (2024).

102. Liu, J. et al. Integration of therapeutic cargo into the human genome with programmable type V-K CAST. *Nat. Commun.* **16**, 2427 (2025).

103. Witte, I. P. et al. Programmable gene insertion in human cells with a laboratory-evolved CRISPR-associated transposase. *Science* **388**, eadt5199 (2025).

104. Anzalone, A. V. et al. Search-and-replace genome editing without double-strand breaks or donor DNA. *Nature* **576**, 149–157 (2019).

105. Zeng, H. et al. Recent advances in prime editing technologies and their promises for therapeutic applications. *Curr. Opin. Biotechnol.* **86**, 103071 (2024).

106. Zhao, Z., Shang, P., Mohanraju, P. & Geijsen, N. Prime editing: advances and therapeutic applications. *Trends Biotechnol.* **41**, 1000–1012 (2023).

107. Shuto, Y. et al. Structural basis for pegRNA-guided reverse transcription by a prime editor. *Nature* **631**, 224–231 (2024).

108. Mathis, N. et al. Predicting prime editing efficiency and product purity by deep learning. *Nat. Biotechnol.* **41**, 1151–1159 (2023).

109. Mathis, N. et al. Machine learning prediction of prime editing efficiency across diverse chromatin contexts. *Nat. Biotechnol.* https://doi.org/10.1038/s41587-024-02268-2 (2024).

110. Yu, G. et al. Prediction of efficiencies for diverse prime editing systems in multiple cell types. *Cell* **186**, 2256–2272 e2223 (2023).

111. Nelson, J. W. et al. Engineered pegRNAs improve prime editing efficiency. *Nat. Biotechnol.* **40**, 402–410 (2022).

112. Song, M. et al. Generation of a more efficient prime editor 2 by addition of the Rad51 DNA-binding domain. *Nat. Commun.* **12**, 5617 (2021).

113. Lee, J. et al. Prime editing with genuine Cas9 nickases minimizes unwanted indels. *Nat. Commun.* **14**, 1786 (2023).

114. Scholefield, J. & Harrison, P. T. Prime editing—an update on the field. *Gene Ther.* **28**, 396–401 (2021).

115. Chen, P. J. et al. Enhanced prime editing systems by manipulating cellular determinants of editing outcomes. *Cell* **184**, 5635–5652 e5629 (2021).

116. Doman, J. L. et al. Phage-assisted evolution and protein engineering yield compact, efficient prime editors. *Cell* **186**, 3983–4002 e3926 (2023).

117. Yan, J. et al. Improving prime editing with an endogenous small RNA-binding protein. *Nature* **628**, 639–647 (2024).

118. Anzalone, A. V. et al. Programmable deletion, replacement, integration and inversion of large DNA sequences with twin prime editing. *Nat. Biotechnol.* **40**, 731–740 (2022).

119. Tao, R. et al. Bi-PE: bi-directional priming improves CRISPR/Cas9 prime editing in mammalian cells. *Nucleic Acids Res.* **50**, 6423–6434 (2022).

120. Zheng, C. et al. Template-jumping prime editing enables large insertion and exon rewriting in vivo. *Nat. Commun.* **14**, 3369 (2023).

121. Choi, J. et al. Precise genomic deletions using paired prime editing. *Nat. Biotechnol.* **40**, 218–226 (2022).

122. Liu, B. et al. A split prime editor with untethered reverse transcriptase and circular RNA template. *Nat. Biotechnol.* **40**, 1388–1393 (2022).

123. She, K. et al. Dual-AAV split prime editor corrects the mutation and phenotype in mice with inherited retinal degeneration. *Signal Transduct. Target Ther.* **8**, 57 (2023).

124. Zheng, C. et al. A flexible split prime editor using truncated reverse transcriptase improves dual-AAV delivery in mouse liver. *Mol. Ther.* **30**, 1343–1351 (2022).

125. Zhi, S. et al. Dual-AAV delivering split prime editor system for in vivo genome editing. *Mol. Ther.* **30**, 283–294 (2022).

126. Yarnall, M. T. N. et al. Drag-and-drop genome insertion of large sequences without double-strand DNA cleavage using CRISPR-directed integrases. *Nat. Biotechnol.* **41**, 500–512 (2023).

127. Pandey, S. et al. Efficient site-specific integration of large genes in mammalian cells via continuously evolved recombinases and prime editing. *Nat. Biomed. Eng.* https://doi.org/10.1038/s41551-024-01227-1 (2024).

128. Hew, B. E. et al. Directed evolution of hyperactive integrases for site specific insertion of transgenes. *Nucleic Acids Res.* **52**, e64 (2024).

129. Hoijer, I. et al. CRISPR–Cas9 induces large structural variants at on-target and off-target sites in vivo that segregate across generations. *Nat. Commun.* **13**, 627 (2022).

130. Hunt, J. M. T., Samson, C. A., Rand, A. D. & Sheppard, H. M. Unintended CRISPR–Cas9 editing outcomes: a review of the detection and prevalence of structural variants generated by gene-editing in human cells. *Hum. Genet.* **142**, 705–720 (2023).

131. Adikusuma, F. et al. Large deletions induced by Cas9 cleavage. *Nature* **560**, E8–E9 (2018).

132. Kim, D. Y., Moon, S. B., Ko, J. H., Kim, Y. S. & Kim, D. Unbiased investigation of specificities of prime editing systems in human cells. *Nucleic Acids Res.* **48**, 10576–10589 (2020).

133. Liang, S. Q. et al. Genome-wide profiling of prime editor off-target sites in vitro and in vivo using PE-tag. *Nat. Methods* **20**, 898–907 (2023).

134. Kleinstiver, B. P. et al. High-fidelity CRISPR–Cas9 nucleases with no detectable genome-wide off-target effects. *Nature* **529**, 490–495 (2016).

135. Slaymaker, I. M. et al. Rationally engineered Cas9 nucleases with improved specificity. *Science* **351**, 84–88 (2016).

136. Casini, A. et al. A highly specific SpCas9 variant is identified by in vivo screening in yeast. *Nat. Biotechnol.* **36**, 265–271 (2018).

137. Ikeda, A., Fujii, W., Sugiura, K. & Naito, K. High-fidelity endonuclease variant HypaCas9 facilitates accurate allele-specific gene modification in mouse zygotes. *Commun. Biol.* **2**, 371 (2019).

138. Chen, J. S. et al. Enhanced proofreading governs CRISPR–Cas9 targeting accuracy. *Nature* **550**, 407–410 (2017).

139. Bessen, J. L. et al. High-resolution specificity profiling and off-target prediction for site-specific DNA recombinases. *Nat. Commun.* **10**, 1937 (2019).

140. Vicencio, J. et al. Genome editing in animals with minimal PAM CRISPR–Cas9 enzymes. *Nat. Commun.* **13**, 2601 (2022).

141. Liang, F. et al. SpG and SpRY variants expand the CRISPR toolbox for genome editing in zebrafish. *Nat. Commun.* **13**, 3421 (2022).

142. Hibshman, G. N. et al. Unraveling the mechanisms of PAMless DNA interrogation by SpRY-Cas9. *Nat. Commun.* **15**, 3663 (2024).

143. Walton, R. T., Christie, K. A., Whittaker, M. N. & Kleinstiver, B. P. Unconstrained genome targeting with near-PAMless engineered CRISPR–Cas9 variants. *Science* **368**, 290–296 (2020).

144. Kweon, J. et al. Engineered prime editors with PAM flexibility. *Mol. Ther.* **29**, 2001–2007 (2021).

145. Oh, Y. et al. Expansion of the prime editing modality with Cas9 from *Francisella novicida*. *Genome Biol.* **23**, 92 (2022).

146. Oh, Y. et al. Highly efficient and specific regulation of gene expression using enhanced CRISPR–Cas12f system. *Gene Ther.* **31**, 358–365 (2024).

147. Sharrar, A. et al. Viral delivery of compact CRISPR–Cas12f for gene editing applications. *CRISPR J.* **7**, 150–155 (2024).

148. Wu, T. et al. An engineered hypercompact CRISPR–Cas12f system with boosted gene-editing activity. *Nat. Chem. Biol.* **19**, 1384–1393 (2023).

149. Wu, Z. et al. Programmed genome editing by a miniature CRISPR–Cas12f nuclease. *Nat. Chem. Biol.* **17**, 1132–1138 (2021).

150. Ennifar, E., Meyer, J. E., Buchholz, F., Stewart, A. F. & Suck, D. Crystal structure of a wild-type Cre recombinase-loxP synapse reveals a novel spacer conformation suggesting an alternative mechanism for DNA cleavage activation. *Nucleic Acids Res.* **31**, 5449–5460 (2003).

151. Jo, C. H. et al. Crystal structure of *Thermoplasma acidophilum* XerA recombinase shows large C-shape clamp conformation and cis-cleavage mode for nucleophilic tyrosine. *FEBS Lett.* **590**, 848–856 (2016).

152. Subramanya, H. S. et al. Crystal structure of the site-specific recombinase, XerD. *EMBO J.* **16**, 5178–5187 (1997).

153. Bebel, A., Karaca, E., Kumar, B., Stark, W. M. & Barabas, O. Structural snapshots of Xer recombination reveal activation by synaptic complex remodeling and DNA bending. *eLife* https://doi.org/10.7554/eLife.19706 (2016).

154. Abbani, M., Iwahara, M. & Clubb, R. T. The structure of the excisionase (Xis) protein from conjugative transposon Tn916 provides insights into the regulation of heterobivalent tyrosine recombinases. *J. Mol. Biol.* **347**, 11–25 (2005).

155. Rutherford, K., Yuan, P., Perry, K., Sharp, R. & Van Duyne, G. D. Attachment site recognition and regulation of directionality by the serine integrases. *Nucleic Acids Res.* **41**, 8341–8356 (2013).

156. Yuan, P., Gupta, K. & Van Duyne, G. D. Tetrameric structure of a serine integrase catalytic domain. *Structure* **16**, 1275–1286 (2008).

157. Qu, Z. et al. Mycobacterial EST12 activates a RACK1-NLRP3-gasdermin D pyroptosis-IL-1beta immune pathway. *Sci. Adv.* https://doi.org/10.1126/sciadv.aba4733 (2020).

158. Headey, S. J. et al. Solution structure and DNA binding of the catalytic domain of the large serine resolvase TnpX. *J. Mol. Recognit.* **28**, 316–324 (2015).

ACKNOWLEDGEMENTS

COMPETING INTERESTS
The authors declare no competing interests.

ADDITIONAL INFORMATION
Correspondence and requests for materials should be addressed to Ho-Joong Kim or Seung Hwan Lee.

Reprints and permission information is available at http://www.nature.com/reprints

Publisher's note Springer Nature remains neutral with regard to jurisdictional claims in published maps and institutional affiliations.